Applied Catalysis B: Environmental 89 (2009) 527–535

Contents lists available at ScienceDirect

Applied Catalysis B: Environmental

journal homepage: www.elsevier.com/locate/apcatb

Decolorization of methylene blue by heterogeneous Fenton reaction using $Fe_{3-x}Ti_xO_4$ ($0 \leq x \leq 0.78$) at neutral pH values

Shijian Yang [a,b], Hongping He [a,*], Daqing Wu [a], Dong Chen [c], Xiaoliang Liang [a,b], Zonghua Qin [a,b], Mingde Fan [a,b], Jianxi Zhu [a], Peng Yuan [a]

[a] Guangzhou Institute of Geochemistry, Chinese Academy of Sciences, Guangzhou 510640, PR China
[b] Graduate School of the Chinese Academy of Sciences, Beijing 100039, PR China
[c] School of Resources & Environmental Engineering, Hefei University of Technology, Hefei 230009, PR China

ARTICLE INFO

Article history:
Received 26 October 2008
Received in revised form 31 December 2008
Accepted 19 January 2009
Available online 29 January 2009

Keywords:
$Fe_{3-x}Ti_xO_4$
Adsorption
Degradation
Mineralization
Zero-order kinetic rate constant

ABSTRACT

In this work, a series of $Fe_{3-x}Ti_xO_4$ ($0 \leq x \leq 0.78$) was synthesized using a new soft chemical method. The synthetic $Fe_{3-x}Ti_xO_4$ were characterized using X-ray diffraction (XRD), Fourier transform infrared spectroscopy (FTIR), Mössbauer spectroscopy, thermogravimetric and differential scanning calorimetry (TG–DSC) analyses. The results showed that they were spinel structures and Ti was introduced into their structures.

Then, decolorization of methylene blue (MB) by $Fe_{3-x}Ti_xO_4$ in the presence of H_2O_2 at neutral pH values was studied using UV–vis spectra, dissolved organic carbon (DOC) and element C analyses. Furthermore, the degradation products remained in reaction solution after the decolorization were identified using ionic chromatography (IC), ^{13}C nuclear magnetic resonance spectra (NMR), liquid chromatography and mass spectrometry (LC–MS). Although small amounts of MB were mineralized, the aromatic rings in MB were destroyed completely after the decolorization. Decolorization of MB by $Fe_{3-x}Ti_xO_4$ in the presence of H_2O_2 was promoted remarkably with the increase of Ti content in $Fe_{3-x}Ti_xO_4$ due to the enhancement of both adsorption and degradation of MB on $Fe_{3-x}Ti_xO_4$.

1. Introduction

Decolorization of synthetic dyes as potential environmental pollutants attracted considerable attention in the past two decades [1]. Two main approaches have been developed for the remediation of dyes containing effluents. One is to utilize various types of microorganisms to degrade synthetic dyes. The use of bioremediation is limited mainly due to the complexity of the biological process that results in a low speed of degradation [1,2]. High degradation rates can only be achieved with purified microbial enzymes, e.g. laccase or peroxidase [3,4]. The other is to utilize many alternative chemical and phys-chemical methods such as, TiO_2 and ZnO photolysis [5–8], ultraviolet light and ultrasonic treatment [9,10], wet air oxidation [11] and ozonization [12]. Most of them are of limited use due to high operation costs and/or the need of special equipments [1].

One of the possible solutions to cope with the problem seems to be the use of catalytic oxidation with hydrogen peroxide (H_2O_2). The most widely used catalytic process for dye degradation is homogeneous Fenton oxidation [13]. But there are some disadvantages for the application of the homogeneous Fenton process, including the requirement of low pH and a significant amount of ferric hydroxide sludge formed in the course of homogeneous Fenton treatment [14,15].

So far, heterogeneous catalysis for decomposing synthetic dyes or other organic compounds by hydrogen peroxide has been described, in which classical heterogeneous Fenton oxidation with iron oxide, Fe-hydroxide or clay-based Fe nanocomposite is employed [16–21]. Unfortunately, the requirement of UV light for photocatalysis, unsuitable pH-dependence of activity, strong iron leaching due to low pH and the difficulty of catalyst recovery [16,17,22] limit the use of these processes for industrial effluents.

Recent studies demonstrate that magnetite is the most effective heterogeneous Fenton catalyst as compared to other iron oxides [23–25], possibly because it is the only one that has Fe^{2+} in its structure to enhance the production rate of $^{\bullet}OH$ [23]. Meanwhile, its inherent magnetism leads it easy to be separated from the reaction system [26,27]. More recently, it is reported that the introduction of Co, Cr and Mn into magnetite structure to form $Fe_{3-x}Co_xO_4$, $Fe_{3-x}Cr_xO_4$ and $Fe_{3-x}Mn_xO_4$ may strongly promote the decolorization of methylene blue (MB) at neutral pH values due to a significant promotion of H_2O_2 decomposition [28–30].

As well known, titanomagnetite ($Fe_{3-x}Ti_xO_4$) is extensively distributed in the crust of earth [31,32]. It is interesting whether

* Corresponding author. Tel.: +86 20 85290257; fax: +86 20 85290130.
E-mail addresses: yangshijiangsq@163.com (S. Yang), hehp@gig.ac.cn (H. He).

0926-3373/$ – see front matter © 2009 Elsevier B.V. All rights reserved.
doi:10.1016/j.apcatb.2009.01.012

the introduction of Ti into magnetite structure also has a remarkable effect on promoting the decolorization of synthetic dyes. Hence, the main aim of this study is to investigate the effect of the introduction of Ti into magnetite structure on the decolorization of synthetic dyes in the presence of H_2O_2 at neutral pH values. MB is a typical synthetic cationic dye, used extensively for dying cotton, wool and silk. The risk of the presence of this dye in waste water may be arisen from the burns effect of eye, nausea, vomiting and diarrhea [33]. So MB was selected as a model pollutant in this study.

2. Experimental

2.1. Synthesis of $Fe_{3-x}Ti_xO_4$

Ferrous sulfate heptahydrate ($FeSO_4{\cdot}7H_2O$), sodium nitrate ($NaNO_3$), titanium tetrachloride ($TiCl_4$), hydrochloric acid (HCl), hydrazine ($N_2H_4{\cdot}H_2O$) and sodium hydroxide (NaOH), which are of analytical grade, were used as received. The procedure of soft chemistry to synthesize $Fe_{3-x}Ti_xO_4$ was as follows:

(1) Suitable amounts of ferrous sulfate and titanium tetrachloride were dissolved in a HCl solution (total metal cation concentration ≈ 0.90 mol L^{-1}). 1.0 mL of hydrazine was added to prevent the oxidation of ferrous cations [34], and pH (<1) was low enough to prevent any titanium or iron oxide and hydroxide precipitation [32].
(2) A solution with 4.0 mol L^{-1} NaOH and 0.90 mol L^{-1} $NaNO_3$ was heated. When the temperature of the solution went up to 90–100 °C, a stoichiometric volume of metal solution was added dropwise (10 mL min^{-1}) into the heating alkaline solution while stirring at a rate of 500 rpm. After dropping, the solution was heated at 90 °C for 1 h. Then, it was cooled to room temperature. It was necessary to emphasize that during the experiment, N_2 was passed through to prevent the oxidation of ferrous cations by air [35].

Various possible summary reactions [36], including intermediate steps, for the synthesis of $Fe_{3-x}Ti_xO_4$ could be written as follows:

$$(3-x)Fe^{2+} + xTi^{4+} + (6+2x)OH^- \rightarrow Fe_{3-x}Ti_x(OH)_{6+2x} \quad (1)$$

$$Fe_{3-x}Ti_x(OH)_{6+2x} + (1-x)NO_3^- \rightarrow Fe_{3-x}Ti_xO_4 + (1-x)NO_2^- + (3+x)H_2O \quad (2)$$

$$Fe_{3-x}Ti_x(OH)_{6+2x} + (2-2x)NO_2^- \rightarrow Fe_{3-x}Ti_xO_4 + (2-2x)NO + (2+2x)H_2O + (2-2x)OH^- \quad (3)$$

$$5Fe_{3-x}Ti_x(OH)_{6+2x} + (2-2x)NO \rightarrow 5Fe_{3-x}Ti_xO_4 + (2-2x)NH_3 + (8x+12)H_2O \quad (4)$$

(3) The particles were then separated by centrifugation at 3500 rpm for 5 min and washed with boiling distilled water under ultrasonication for 5 min followed by a new centrifugation [32]. After four washings, the particles were collected and dried in a vacuum oven at 100 °C for 24 h.

Fe_3O_4 was synthesized with this procedure in the absence of titanic cations [35,36].

2.2. Characterization

Contents of Fe and Ti in synthetic $Fe_{3-x}Ti_xO_4$ were measured spectrophotometrically with the phenanthroline method and diantipyrylmethane method, respectively. The chemical formula of synthetic $Fe_{3-x}Ti_xO_4$ was calculated with the results of chemical analysis using:

$$x = \frac{55.848 \times 3 \times C_{Ti}}{47.868 \times C_{Fe} + 55.848 \times C_{Ti}} \quad (5)$$

where C_{Fe} and C_{Ti} are the contents of Fe and Ti in synthetic $Fe_{3-x}Ti_xO_4$, respectively.

Powder X-ray diffraction patterns (XRD) were recorded between 10° and 80° at a step of 1° min^{-1}, using a Bruker D8 advance diffractometer with Cu Kα radiation (40 kV and 40 mA).

Fourier transform infrared spectra (FTIR) were recorded on Vector 33 Fourier transform infrared spectrometer. 64 scans were collected for each measurement in the spectral range of 400–4000 cm^{-1} with a resolution of 4 cm^{-1}. Specimens for measurement were prepared by mixed 5 mg of the sample powder with 95 mg of KBr and by pressing the mixture into a pellet.

Thermogravimetric and differential scanning calorimetry (TG–DSC) analyses were synchronously performed on a Netzsch STA 409PC Instrument. About 20 mg of finely ground sample was heated in a corundum crucible from 30 to 800 °C at a heating rate of 5 °C min^{-1} under high pure N_2 or air atmosphere (60 cm^3 min^{-1}).

Mössbauer effect measurements were carried out on a spectrometer (assembled by Wissel et al., in Nanjing University, PR China) with a $^{57}Co/Pd$ source at room temperature using α-Fe as reference, proportional counter. The γ-ray was oriented perpendicular to the sample.

2.3. Adsorption isotherm

Batch adsorption studies of MB on synthetic $Fe_{3-x}Ti_xO_4$ at pH 6.8 were carried out in glass vessels with agitation provided by a shaker [37]. The temperature was controlled at 25 °C by air bath. The pH values were adjusted to pH 6.8 using a buffer solution (KH_2PO_4 + NaOH). It was proved by FTIR spectra that little phosphate adsorbed on $Fe_{3-x}Ti_xO_4$ at pH 6.8. The suspension containing 60.0 mg of dry $Fe_{3-x}Ti_xO_4$ and 20.0 mL of varying concentrations of MB (20–400 mg L^{-1}) was shaken on an orbit shaker at 200 rpm. The system was agitated for a sufficient time (24 h) to reach equilibrium. Then, $Fe_{3-x}Ti_xO_4$ were separated by centrifugation and the amount of MB retained on per gram of $Fe_{3-x}Ti_xO_4$ at equilibrium (q_e) was calculated using:

$$q_e = (C_i - C_e)\frac{V}{m} \quad (6)$$

where C_i and C_e are the initial and equilibrium concentrations of MB in aqueous solution, respectively.

2.4. Decolorization reaction

The decolorization of MB (C_0 = 100 mg L^{-1}) by synthetic $Fe_{3-x}Ti_xO_4$ in the presence of H_2O_2 (0.30 mol L^{-1}) [28–30] and in the absence of H_2O_2 at pH 6.8 and room temperature was carried out in a glass reactor (containing 400 mL of reaction solution) equipped with a magnetic stirrer. The reaction was started by the addition of MB or H_2O_2. During the reaction, the magnetic stirrer stirred at a rate of 500 rpm and little $Fe_{3-x}Ti_xO_4$ adhered to the magnetic stirrer. At each sampling time, 5 mL of reaction solution was sampled from the reactor. Immediately, $Fe_{3-x}Ti_xO_4$ was separated by centrifugation at 3500 rpm for 3 min. 2.0 mL of the supernatant was sampled and diluted for dissolved organic carbon (DOC) and UV–vis analyses. The separated $Fe_{3-x}Ti_xO_4$ was dried in a vacuum oven at 100 °C for 24 h for the analysis of element C. It was decided not to stop the reaction by the addition of a quenching agent because this interfered with the analysis of the reaction mixture [1]. In the experiments with the pH-dependence, the pH

values of reaction systems were adjusted to pH 6.8 using the buffer solution (KH_2PO_4 + NaOH). The degree of MB removed from reaction solution was expressed as the percent decrease of absorbance at absorption maximum of 665 nm. During the decolorization, DOC in reaction solution was determined using a Shimadzu TOC-V_{CPH} analyzer, and element C content on dry $Fe_{3-x}Ti_xO_4$ was examined using a Vario EL III element analyzer. After the decolorization, the concentrations of nitrate, sulfate and ammonium ions in reaction solution were determined using ionic chromatography (DX-600) and Nessler's reagent colorimetic method, respectively. The organic compounds in reaction solution after the decolorization were examined using ^{13}C nuclear magnetic resonance spectra (NMR), liquid chromatography and mass spectrometry (LC–MS). ^{13}C NMR was obtained with a Bruker AVANCE Digital 400 MHz NMR spectrometer. Samples of ^{13}C NMR were prepared as follows [38]: after the decolorization, $Fe_{3-x}Ti_xO_4$ was removed by centrifugation. Subsequently, the supernatant (200 mL) was freeze-dried to remove the water. The remaining residue was dissolved in 0.5 mL of D_2O. LC–MS was operated on an API 4000 LC–MS.

3. Results and discussion

3.1. Characterization of synthetic $Fe_{3-x}Ti_xO_4$

3.1.1. Chemical analysis

The results of chemical analysis are shown in Table 1. The chemical formula of synthetic $Fe_{3-x}Ti_xO_4$ can be notated as Fe_3O_4, $Fe_{2.83}Ti_{0.17}O_4$, $Fe_{2.77}Ti_{0.23}O_4$, $Fe_{2.63}Ti_{0.37}O_4$, $Fe_{2.50}Ti_{0.50}O_4$ and $Fe_{2.22}Ti_{0.78}O_4$, respectively.

3.1.2. XRD

XRD patterns of synthetic $Fe_{3-x}Ti_xO_4$ are shown in Fig. 1A. The characteristic peaks of them correspond very well to the standard card of magnetite (JCPDS: 19-0629). It indicates that synthetic $Fe_{3-x}Ti_xO_4$ was spinel structure.

To show the hyperfine structural characteristics of synthetic $Fe_{3-x}Ti_xO_4$, the expansion of the diffraction lines at ca. 35.5° is shown in Fig. 1B. The lattice parameter of synthetic Fe_3O_4 was 0.840 nm. It indicates that synthetic Fe_3O_4 was pure phase magnetite. As the radius of Ti^{4+} (0.68 Å) is larger than Fe^{3+} (0.64 Å), the lattice parameter of titanomagnetite is greater than magnetite [32]. The lattice parameters of synthetic $Fe_{2.77}Ti_{0.23}O_4$, $Fe_{2.50}Ti_{0.50}O_4$ and $Fe_{2.22}Ti_{0.78}O_4$ were 0.842, 0.843 and 0.842 nm respectively, which were all greater than magnetite. So for synthetic $Fe_{3-x}Ti_xO_4$ ($x \neq 0$), Ti was introduced into their structures. The lattice parameter of synthetic $Fe_{2.77}Ti_{0.23}O_4$ was very close to the theoretical value [39]. It indicates that synthetic $Fe_{2.77}Ti_{0.23}O_4$ was pure phase $Fe_{2.77}Ti_{0.23}O_4$. But the lattice parameters of synthetic $Fe_{2.50}Ti_{0.50}O_4$ and $Fe_{2.22}Ti_{0.78}O_4$ were much less than the theoretical values of them (0.846 nm for $Fe_{2.50}Ti_{0.50}O_4$, and 0.851 nm for $Fe_{2.22}Ti_{0.78}O_4$) [39]. It may be attributed to the partial oxidation of Fe^{2+} ions, or the presence of amorphous TiO_2 in synthetic $Fe_{2.50}Ti_{0.50}O_4$ and $Fe_{2.22}Ti_{0.78}O_4$.

Table 1
Fe and Ti contents in synthetic $Fe_{3-x}Ti_xO_4$.

$Fe_{3-x}Ti_xO_4$	Chemical analyses (wt%)	
	Fe	Ti
$x = 0$	67.9	0
$x = 0.17$	65.0	3.25
$x = 0.23$	65.4	4.72
$x = 0.37$	58.4	6.98
$x = 0.50$	55.1	9.38
$x = 0.78$	46.4	14.1

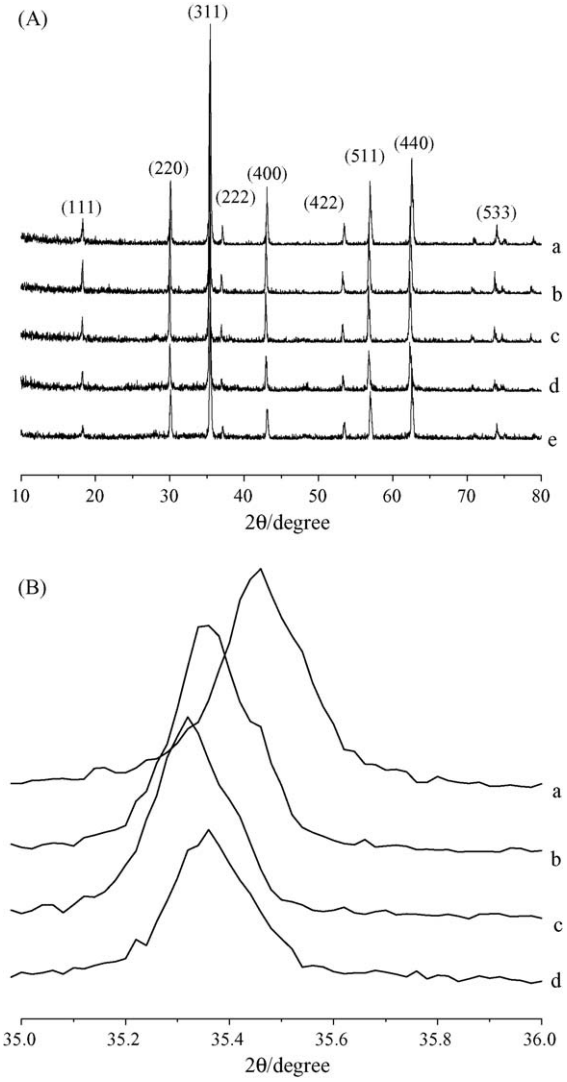

Fig. 1. XRD patterns of (A) synthetic $Fe_{3-x}Ti_xO_4$; (B) expansion of the diffraction lines at ca. 35.5°. (a) $x = 0$; (b) $x = 0.23$; (c) $x = 0.50$; (d) $x = 0.78$; (e) $x = 0.78$ after calcination.

To exclude the presence of amorphous TiO_2, synthetic $Fe_{2.22}Ti_{0.78}O_4$ was calcined under N_2 atmosphere at 400 °C for 8 h. XRD pattern of synthetic $Fe_{2.22}Ti_{0.78}O_4$ after calcination was recorded (shown in Fig. 1A(e)). If there were some amorphous TiO_2 in synthetic $Fe_{2.22}Ti_{0.78}O_4$, amorphous TiO_2 would be transformed into rutile (or anatase) after calcination. As shown in Fig. 1A(e), the characteristic peaks corresponding to rutile or anatase did not appear. So there was no amorphous TiO_2 in synthetic $Fe_{2.22}Ti_{0.78}O_4$ and the less of lattice parameter was attributed to the partial oxidation of Fe^{2+} ions happened in synthetic $Fe_{2.22}Ti_{0.78}O_4$.

Crystal sizes of synthetic $Fe_{3-x}Ti_xO_4$ were calculated with the Scherrer's equation [40]. The average diameters of them were all about 120 nm.

3.1.3. FTIR

Infrared spectra of synthetic $Fe_{3-x}Ti_xO_4$ are shown in Fig. 2. The infrared spectra showed characteristic bands at about 470, 585 and 890 cm^{-1}. The band at about 585 cm^{-1} is the characteristic vibration of magnetite [41,42] and the vibration at about 470 cm^{-1} may be attributed to the introduction of Ti into magnetite structure. The vibration at about 890 cm^{-1} is ascribed to OH bending mode [43]. It was suggested that a small amount of –OH in synthetic magnetite was a prerequisite for the formation of

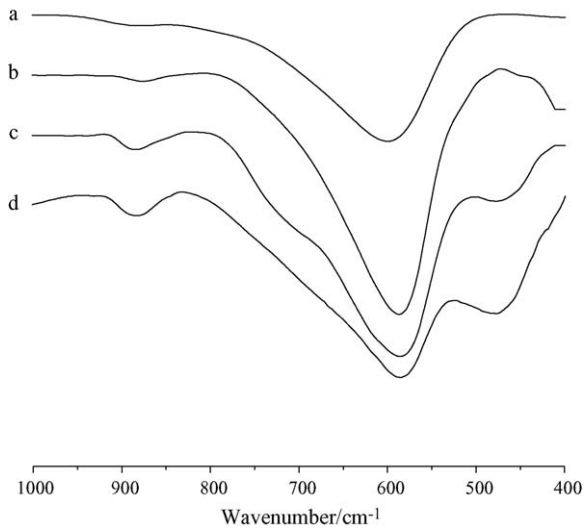

Fig. 2. FTIR spectra of synthetic $Fe_{3-x}Ti_xO_4$: (a) $x = 0$; (b) $x = 0.23$; (c) $x = 0.50$; (d) $x = 0.78$.

maghemite [34,44]. It can be observed that the intensity of this vibration enhanced with the increase of Ti content in synthetic $Fe_{3-x}Ti_xO_4$.

3.1.4. Mössbauer spectra

Room temperature Mössbauer measurement (Fig. 3) showed typical spectra, suggesting the presence of the cubic spinel phase. The fitted Mössbauer parameters are displayed in Table 2. Mössbauer spectra of synthetic Fe_3O_4 contained two distinct hyperfine components with areal fractions of about 1:2 ratio. The sextet with 49.0 T hyperfine magnetic field (HMF) and 0.30 mm s^{-1} isomer shift (IS) (relative to pure α-Fe) corresponds to the A-site Fe^{3+} ions. The large sextet with HMF = 46.0 T and IS = 0.66 mm s^{-1} is related to the B-site $Fe^{2.5+}$ ions, which arise from the rapid electron exchange between Fe^{2+} and Fe^{3+} ions [45]. These are the standard characteristics of pure phase magnetite. As Ti was introduced into magnetite structure, a strong effect on Mössbauer spectra can be observed. For magnetite, if one Fe^{3+} cation is replaced by Ti^{4+} cation, another Fe^{3+} cation will be converted to Fe^{2+} cation to compensate the valence difference between Ti^{4+} and Fe^{3+} cations [46]. Comparing synthetic $Fe_{2.83}Ti_{0.17}O_4$ with Fe_3O_4, no change happened in the A-site except relative spectra area (RA), but pronounced changes including IS and RA happened in the B-site (shown in Table 2). It indicates that for synthetic $Fe_{2.83}Ti_{0.17}O_4$, Ti selectively entered the B-site and the conversion of Fe^{3+} to Fe^{2+} only happened in the B-site [46]. With the increase of Ti content, a new component (labeled C in Table 2) appeared under the shoulder of the sextet external peaks (shown in Fig. 3c–e) and its RA increased (shown in Table 2). This phenomenon was also reported by previous research on titanomagnetite [45]. Pronounced changes including IS, HMF and RA happened in the B-site. Furthermore, slight changes including IS and HMF happened in the A-site. It may indicate that for synthetic $Fe_{2.63}Ti_{0.37}O_4$, $Fe_{2.50}Ti_{0.50}O_4$ and $Fe_{2.22}Ti_{0.78}O_4$, Ti still selectively entered the B-site, but the conversion of Fe^{3+} to Fe^{2+} happened in both the A-site and B-site [46].

Table 2
Hyperfine room temperature Mössbauer parameters of synthetic $Fe_{3-x}Ti_xO_4$.

$Fe_{3-x}Ti_xO_4$	Assign	IS (mm s^{-1})	HMF (T)	ε, Δ (mm s^{-1})	RA
$x = 0$	A	0.30	49.0	0.00	0.34
	B	0.66	46.0	−0.02	0.66
$x = 0.17$	A	0.30	49.0	0.00	0.45
	B	0.56	45.7	−0.02	0.55
$x = 0.37$	A	0.32	48.1	−0.02	0.39
	B	0.60	44.3	0	0.53
	C	0.80	–	0.92	0.08
$x = 0.50$	A	0.32	48.1	−0.02	0.41
	B	0.59	44.2	0.00	0.49
	C	0.83	–	0.82	0.10
$x = 0.78$	A	0.33	47.9	0.02	0.35
	B	0.59	44.0	−0.02	0.54
	C	0.34	–	0.41	0.11

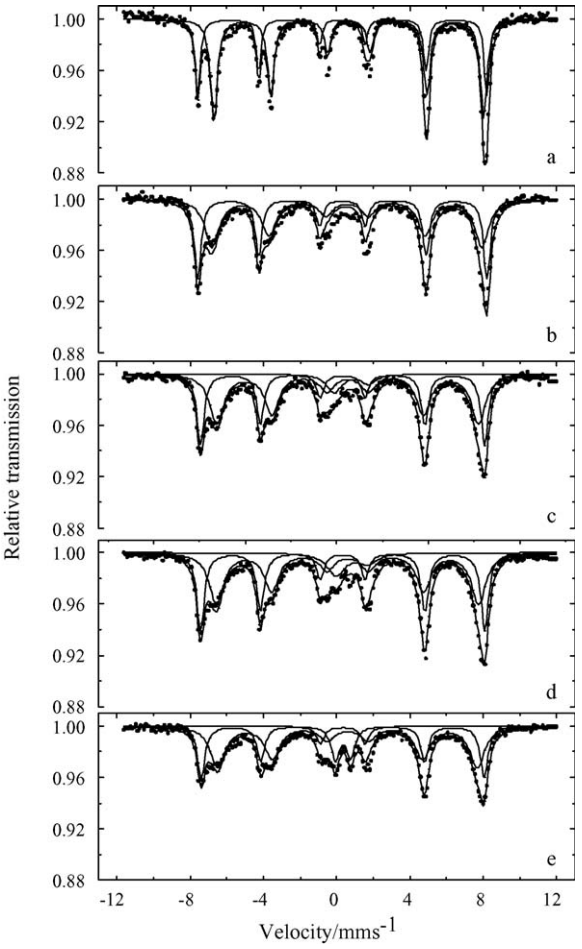

Fig. 3. Room temperature Mössbauer spectra of synthetic $Fe_{3-x}Ti_xO_4$: (a) $x = 0$; (b) $x = 0.17$; (c) $x = 0.37$; (d) $x = 0.50$; (e) $x = 0.78$.

3.1.5. TG–DSC

TG analyses for synthetic $Fe_{3-x}Ti_xO_4$ under air atmosphere showed weight gains from about 150–400 °C (shown in Fig. 4). It indicates that there were some Fe^{2+} cations in synthetic $Fe_{3-x}Ti_xO_4$. But the observed weight gains were less than the theoretical values to produce titanomaghemite (or maghemite). Weight losses due to dehydroxylation and dehydration [47] were observed from about 30–350 °C in the TG curves of synthetic $Fe_{3-x}Ti_xO_4$ under N_2 atmosphere (shown in Fig. 5). For synthetic Fe_3O_4 and $Fe_{2.77}Ti_{0.23}O_4$, the sums of the weight gains (in Fig. 4) and the weight losses (in Fig. 5) were very close to the theoretical weight gains. It indicates that for synthetic Fe_3O_4 and $Fe_{2.77}Ti_{0.23}O_4$, the less weight gains under air atmosphere were attributed to the dehydroxylation and dehydration during oxidation. Taking account of the effect of dehydroxylation and dehydration, the weight gains of synthetic $Fe_{2.50}Ti_{0.50}O_4$ and $Fe_{2.22}Ti_{0.78}O_4$ were still

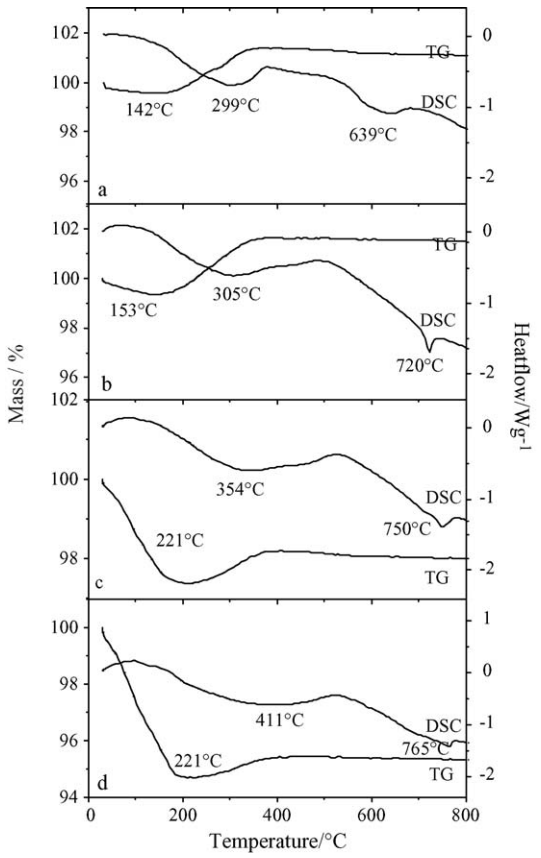

Fig. 4. TG–DSC curves of synthetic $Fe_{3-x}Ti_xO_4$ under air atmosphere: (a) $x = 0$; (b) $x = 0.23$; (c) $x = 0.50$; (d) $x = 0.78$.

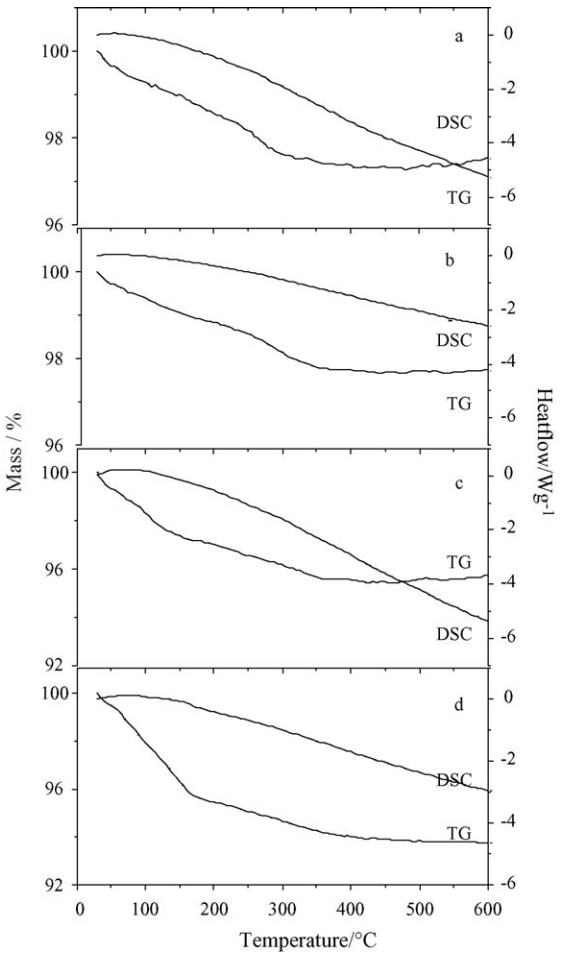

Fig. 5. TG–DSC curves of synthetic $Fe_{3-x}Ti_xO_4$ under N_2 atmosphere: (a) $x = 0$; (b) $x = 0.23$; (c) $x = 0.50$; (d) $x = 0.78$.

less than the theoretical values. It indicates that some Fe^{2+} ions in synthetic $Fe_{2.50}Ti_{0.50}O_4$ and $Fe_{2.22}Ti_{0.78}O_4$ were oxidized during preparation. This result is consistent with XRD analysis.

There were no obvious peaks appeared in the DSC curves of synthetic $Fe_{3-x}Ti_xO_4$ under N_2 atmosphere (shown in Fig. 5). It indicates that no obvious phase transition happened in synthetic $Fe_{3-x}Ti_xO_4$ during the heating under N_2 atmosphere. It is consistent with XRD analysis of synthetic $Fe_{2.22}Ti_{0.78}O_4$ after calcination. As shown in Fig. 4, DSC curves of synthetic $Fe_{3-x}Ti_xO_4$ under air atmosphere showed two obvious exothermic peaks. The exothermic peak centered at about 300–400 °C corresponds well to the TG weight gain. So it may be attributed to the oxidation of Fe^{2+} ions. It is interesting to observe that with the increase of Ti content in synthetic $Fe_{3-x}Ti_xO_4$, the oxidation temperature gradually increased. It indicates that the introduction of Ti into magnetite structure restrained the further oxidation of magnetite to maghemite. Another exothermic peak centered at about 600–800 °C may be related to the phase transition of maghemite to hematite [28]. It is interesting to observe that as the Ti content in synthetic $Fe_{3-x}Ti_xO_4$ increased, the transition temperature gradually increased. It indicates that the introduction of Ti had a stabilization effect on the spinel structure.

3.2. Decolorization of MB by $Fe_{3-x}Ti_xO_4$

Decolorization of MB by synthetic $Fe_{3-x}Ti_xO_4$ in the presence of H_2O_2 was tested (shown in Fig. 6). It can be seen that the residual MB in reaction solutions decreased with the increase of Ti content in $Fe_{3-x}Ti_xO_4$. After the addition of H_2O_2 and MB into reaction solutions for 1 h, about 20%, 29%, 65% and 90% of MB had been removed by Fe_3O_4, $Fe_{2.77}Ti_{0.23}O_4$, $Fe_{2.50}Ti_{0.50}O_4$ and $Fe_{2.22}Ti_{0.78}O_4$, respectively. After 24 h, about 79%, 92%, 98% and 98% of MB had been removed by Fe_3O_4, $Fe_{2.77}Ti_{0.23}O_4$, $Fe_{2.50}Ti_{0.50}O_4$ and $Fe_{2.22}Ti_{0.78}O_4$, respectively.

3.2.1. Decolorization process study with UV–vis spectra

The temporal evolution of UV–vis spectra taking place during the decolorization of MB by $Fe_{2.22}Ti_{0.78}O_4$ in the presence of H_2O_2 is displayed in Fig. 7a. Because of the intense absorption of H_2O_2 at about 200 nm, some slight changes in UV–vis spectra during the

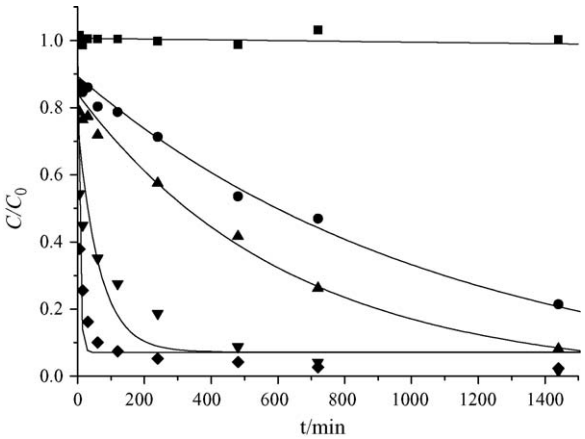

Fig. 6. Decolorization of MB by $Fe_{3-x}Ti_xO_4$ (3.0 g L^{-1}) in the presence of H_2O_2: (■) blank experiment (MB + H_2O_2); (●) $x = 0$; (▲) $x = 0.23$; (▼) $x = 0.50$; (◆) $x = 0.78$.

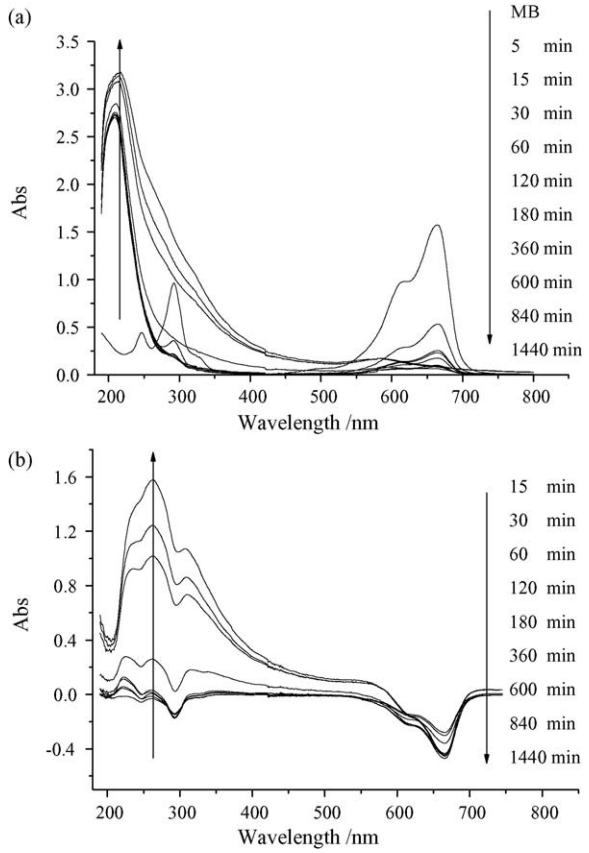

Fig. 7. (a) UV–vis spectra during the decolorization of MB by $Fe_{2.22}Ti_{0.78}O_4$ in the presence of H_2O_2; (b) transformation of a (the spectrum line corresponding to 5 min was subtracted as a baseline from all spectrum lines).

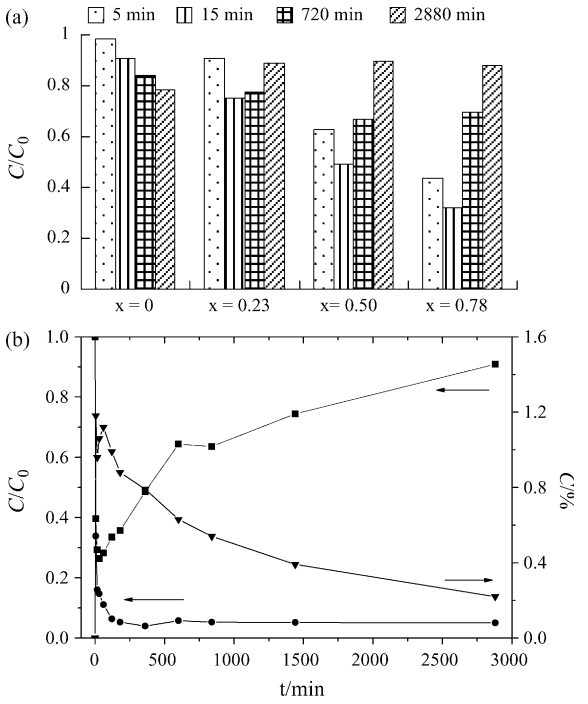

Fig. 8. (a) DOC changes during the decolorization of MB by $Fe_{3-x}Ti_xO_4$ in the presence of H_2O_2; (b) changes of DOC, MB in reaction solution and element C on $Fe_{2.22}Ti_{0.78}O_4$ during the decolorization of MB by $Fe_{2.22}Ti_{0.78}O_4$ in the presence of H_2O_2: (■) DOC; (●) MB; (▼) element C.

decolorization were difficult to be observed. Hence, the spectrum line corresponding to 5 min was used as a baseline and subtracted from all spectrum lines. After this treatment, Fig. 7a was transformed to Fig. 7b. The positive peaks in Fig. 7b indicate that some new compounds appeared, and the negative peaks correspond to the decrease of MB or H_2O_2. The negative peaks at 247, 292 and 665 nm correspond to the removal of MB, and the negative peak at about 200 nm corresponds to the decomposition of H_2O_2. Meanwhile, some positive peaks at 220, 265 and 310 nm were observed. The occurrence of the peak at 220 nm implies the formation of NO_3^-, which was further proved by ionic chromatography. The peak at 265 nm may be ascribed to the appearance of another degradation product. The peak at 310 nm may be attributed to the superposition of the positive peak at 265 nm and the negative peak at 292 nm. So it can be concluded with the appearance of degradation products that some MB was degraded during the decolorization.

3.2.2. Mineralization of MB

To investigate the mineralization during the decolorization of MB by $Fe_{3-x}Ti_xO_4$ in the presence of H_2O_2, changes of DOC in reaction solutions were recorded (shown in Fig. 8a). DOC value reflects the total amount of dissolved organics in reaction solution. It is surprising that for $Fe_{3-x}Ti_xO_4$ ($x \neq 0$), DOC decreased at the beginning, but it turned back gradually. To explain this phenomenon, element C content on $Fe_{3-x}Ti_xO_4$ was determined, which presents the total amount of organics adsorbed on $Fe_{3-x}Ti_xO_4$. Changes of DOC, MB in reaction solution and element C on $Fe_{2.22}Ti_{0.78}O_4$ during the decolorization of MB by $Fe_{2.22}Ti_{0.78}O_4$ in the presence of H_2O_2 are displayed in Fig. 8b. The concentrations of DOC and MB in reaction solution decreased and the content of element C on $Fe_{2.22}Ti_{0.78}O_4$ increased rapidly at the first 15 min. It is mainly attributed to the adsorption of MB on $Fe_{2.22}Ti_{0.78}O_4$. However, the content of element C on $Fe_{2.22}Ti_{0.78}O_4$ decreased and DOC in the solution increased gradually after 30 min. It may be largely attributed to the weak affinity of $Fe_{2.22}Ti_{0.78}O_4$ for the organic degradation products at neutral pH values. As a result, the organic degradation products desorbed from $Fe_{2.22}Ti_{0.78}O_4$ and entered the solution after the degradation of MB on $Fe_{2.22}Ti_{0.78}O_4$. So it can be concluded that small amounts of MB were mineralized during the decolorization.

3.2.3. Determination of degradation product

The deaminization and desulfonication processes during the decolorization occurred as evidenced by the formation of NO_3^-, NH_4^+ and SO_4^{2-}. The concentrations of NO_3^-, NH_4^+ and SO_4^{2-} in reaction solution after the decolorization were 21.4, 6.86 and 22.6 mg L^{-1}, respectively.

The organic compounds in reaction solution after the decolorization were identified using LC–MS spectroscopy. Mass spectra analysis confirms that acetic acid formed and the intermediates proposed in previous researches on the degradation of MB [48–50] did not appear.

Further supporting evidence was obtained using ^{13}C NMR spectroscopy. As shown in Fig. 9, the signal corresponding to carbon atoms in aromatic ring did not appear, leaving two peaks at 171.0 and 34.6 ppm, which correspond to carboxyl and methyl groups in the degradation products, respectively. The NMR findings indicate that the aromatic rings in MB were destroyed completely and small molecules formed.

3.3. Effect of Ti in $Fe_{3-x}Ti_xO_4$ on the decolorization of MB

As shown in Fig. 6, the decolorization of MB by synthetic $Fe_{3-x}Ti_xO_4$ in the presence of H_2O_2 was promoted remarkably with

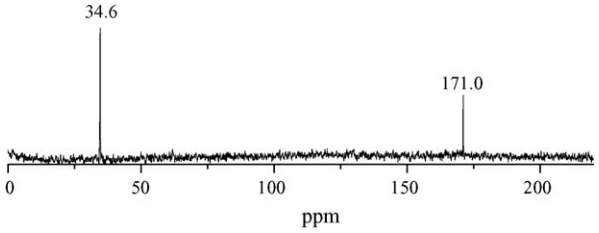

Fig. 9. ^{13}C NMR spectra of the compounds remained in reaction solution after the decolorization.

the increase of Ti content in $Fe_{3-x}Ti_xO_4$. In this instance, the decolorization may result from both adsorption and degradation of MB on $Fe_{3-x}Ti_xO_4$. So the effects of Ti in $Fe_{3-x}Ti_xO_4$ on both adsorption and degradation of MB on $Fe_{3-x}Ti_xO_4$ were investigated.

3.3.1. Effect of Ti in $Fe_{3-x}Ti_xO_4$ on the adsorption of MB

Adsorption of MB on $Fe_{3-x}Ti_xO_4$ was investigated (shown Fig. 10a). After 24 h, about 16%, 23%, 54% and 91% of MB were adsorbed on Fe_3O_4, $Fe_{2.77}Ti_{0.23}O_4$, $Fe_{2.50}Ti_{0.50}O_4$ and $Fe_{2.22}Ti_{0.78}O_4$, respectively. It indicates that the adsorption of MB on synthetic $Fe_{3-x}Ti_xO_4$ was promoted remarkably with the increase of Ti content in $Fe_{3-x}Ti_xO_4$.

Adsorption capacity at different aqueous equilibrium concentration can be illustrated by the adsorption isotherm [37]. The adsorption isotherms of MB on $Fe_{3-x}Ti_xO_4$ at pH 6.8 and 25 °C are showed in Fig. 10b. The adsorption data were fitted to Langmuir adsorption model:

$$q_e = \frac{q_m k_L C_e}{1 + k_L C_e} \quad (7)$$

where q_m is the maximum adsorption capacity and k_L is the equilibrium adsorption constant.

Langmuir isotherm model constants for MB adsorption on $Fe_{3-x}Ti_xO_4$ are displayed in Table 3. It can be seen that the calculated q_m increased remarkably with the increase of Ti content in $Fe_{3-x}Ti_xO_4$. It also demonstrates that with the increase of Ti content in $Fe_{3-x}Ti_xO_4$, the adsorption of MB on synthetic $Fe_{3-x}Ti_xO_4$ was promoted remarkably.

Table 3
Langmuir isotherm model constants for MB adsorption on $Fe_{3-x}Ti_xO_4$.

$Fe_{3-x}Ti_xO_4$	q_m (mg g^{-1})	K_L (L mg^{-1})	R^2
$x = 0$	4.66	0.093	0.7731
$x = 0.23$	5.91	0.082	0.9434
$x = 0.50$	18.2	0.091	0.9821
$x = 0.78$	42.0	0.177	0.9247

3.3.2. Effect of Ti in $Fe_{3-x}Ti_xO_4$ on the degradation of MB

To describe the degradation of MB clearly, another experiment was conducted. In the experiment, H_2O_2 was added after the addition of MB into reaction solution for 12 h. As shown in Fig. 11, the removal of MB before the addition of H_2O_2 (time zero) should be attributed to the adsorption of MB on $Fe_{3-x}Ti_xO_4$, and the further removal of MB after the addition of H_2O_2 should be attributed to the degradation of MB on $Fe_{3-x}Ti_xO_4$.

For iron oxides, its water-wet surface is covered by hydroxyl groups, and these hydroxyl moieties can undergo proton-exchange reactions with the aqueous solution much like dissolved acids [51]. So the adsorption of cationic synthetic dye MB on $Fe_{3-x}Ti_xO_4$ can be described as:

$$\equiv M{-}OH + MB^+ \rightarrow \equiv M{-}OMB + H^+ \quad (8)$$

$\equiv M$ stands for the cation of Fe^{2+}, Fe^{3+} or Ti^{4+} on the surface of $Fe_{3-x}Ti_xO_4$. And the mechanism of MB degradation on $Fe_{3-x}Ti_xO_4$ in the presence of H_2O_2 may be attributed to the radical mechanism [52–57]:

$$\equiv Fe^{III} + H_2O_2 \rightarrow \equiv Fe^{III}H_2O_2 \quad (9)$$

$$\equiv Fe^{III}H_2O_2 \rightarrow \equiv Fe^{II} + {}^{\bullet}HO_2 + H^+ \quad (10)$$

$$\equiv Fe^{II} + H_2O_2 \rightarrow \equiv Fe^{III} + {}^{\bullet}OH + OH^- \quad (11)$$

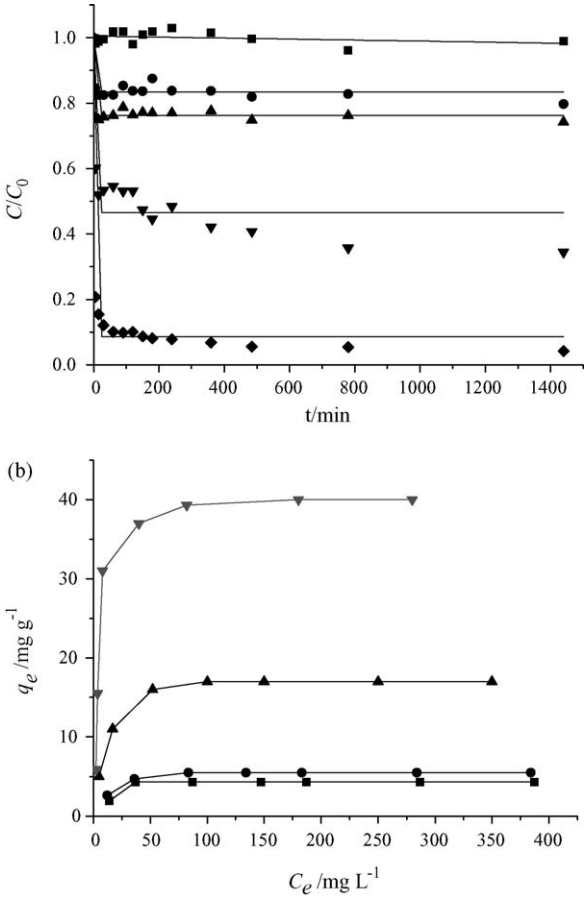

Fig. 10. (a) Adsorption of MB on $Fe_{3-x}Ti_xO_4$ (3.0 g L^{-1}): (■) blank experiment (MB); (●) $x = 0$; (▲) $x = 0.23$; (▼) $x = 0.50$; (◆) $x = 0.78$. (b) Adsorption isotherm of MB on $Fe_{3-x}Ti_xO_4$: (■) $x = 0$; (●) $x = 0.23$; (▲) $x = 0.50$; (▼) $x = 0.78$.

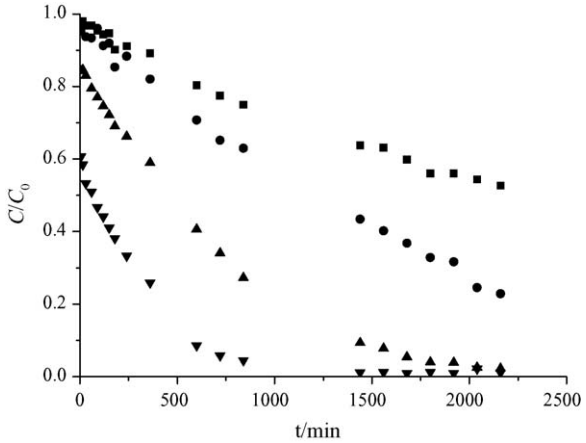

Fig. 11. Degradation of MB on $Fe_{3-x}Ti_xO_4$ (1.0 g L^{-1}): (■) $x = 0$; (●) $x = 0.23$; (▲) $x = 0.50$; (▼) $x = 0.78$.

In these reactions, a hydroxyl radical intermediate is generated, which can decompose MB adsorbed on $Fe_{3-x}Ti_xO_4$. The degradation reaction can be described as:

$$\equiv M-OMB + n^{\bullet}OH \rightarrow \text{products} \quad (12)$$

The kinetic equation of reaction (12) can be expressed as:

$$-\frac{d[\equiv M-OMB]}{dt} = -\frac{n\,d[^{\bullet}OH]}{dt} = k_1[\equiv M-OMB][^{\bullet}OH]^n \quad (13)$$

The production rate of $^{\bullet}OH$ is proportional to the product of $[\equiv Fe]_{total}$ and $[H_2O_2]$ [56]. Because the dissolution of $Fe_{3-x}Ti_xO_4$ at pH 6.8 can be neglected (proved by the experiments), $[\equiv Fe]_{total}$ can be regarded as a constant during the reaction for a particular $Fe_{3-x}Ti_xO_4$. In this experiment, the addition of H_2O_2 (0.30 mol L^{-1}) was much more superfluous for the degradation of MB (100 mg L^{-1}). During the degradation of MB, the reduction of H_2O_2 may be neglected. So $[H_2O_2]$ may be regarded as a constant approximately. As a result, $[^{\bullet}OH]$ in Eq. (13) may be regarded as a constant. When the concentration of MB is sufficiently high in reaction solution for the surface of $Fe_{3-x}Ti_xO_4$ to be saturated with adsorbed MB, [≡M–OMB] will be a constant and equal to q_m. So in this instance, the degradation of MB will follow a zero-order kinetic rate law and Eq. (13) can be transformed as:

$$-\frac{dC}{dt} = k \quad (14)$$

and

$$k = k_1 q_m [^{\bullet}OH]^n \quad (15)$$

so

$$C = C_0' - kt \quad (16)$$

where k is observed zero-order kinetic rate constant; C and C_0' are the concentrations of MB in reaction solution at any time t and time zero. The values of k and $C_0 - C_0'$ may be used to characterize the degradation rate and q_m, respectively.

When the concentration of MB is low in reaction solution for the surface of $Fe_{3-x}Ti_xO_4$ to be saturated with adsorbed MB, [≡M–OMB] will be less than q_m, and decrease gradually during the degradation. In this instance, the fit of the data will deviate from the straight, and the degradation of MB may follow a first-order kinetic rate law. It is regarded that the fit of the data will be a straight when the concentration of MB in reaction solution is higher than $C_0 - C_0'$.

The parameters k and C_0'/C_0 of MB degradation on $Fe_{3-x}Ti_xO_4$ (Fig. 11) were calculated. As shown in Table 4, zero-order kinetic rate constant k increased remarkably with the increase of Ti content in $Fe_{3-x}Ti_xO_4$. It indicates that the degradation of MB on $Fe_{3-x}Ti_xO_4$ was promoted remarkably with the increase of Ti content in $Fe_{3-x}Ti_xO_4$.

After transformation, Eq. (15) can be described as:

$$\frac{k}{q_m} = k_1[^{\bullet}OH]^n \quad (17)$$

The correlation of k with $1 - (C_0'/C_0)$ is displayed in Fig. 12. The fit of the data deviated from a straight and the increase of k lagged behind $1 - (C_0'/C_0)$. As shown in Eq. (17), the slope in Fig. 12 is proportional to $[^{\bullet}OH]^n$. So with the increase of Ti content in $Fe_{3-x}Ti_xO_4$, the production rate of $^{\bullet}OH$ decreased. It may indicate that Ti in $Fe_{3-x}Ti_xO_4$ may not participate in the heterogeneous Fenton reaction. This result is similar to previous research on $Fe_{3-x}Ni_xO_4$ [30].

Table 4
Zero-order kinetic parameters of MB degradation on $Fe_{3-x}Ti_xO_4$.

$Fe_{3-x}Ti_xO_4$	k (min^{-1})	C_0'/C_0	R^2	Applied stage
$x = 0$	0.000215	0.964	0.9877	All
$x = 0.23$	0.000345	0.949	0.9925	All
$x = 0.50$	0.000690	0.836	0.9957	Before 840 min
$x = 0.78$	0.001231	0.592	0.9675	Before 180 min

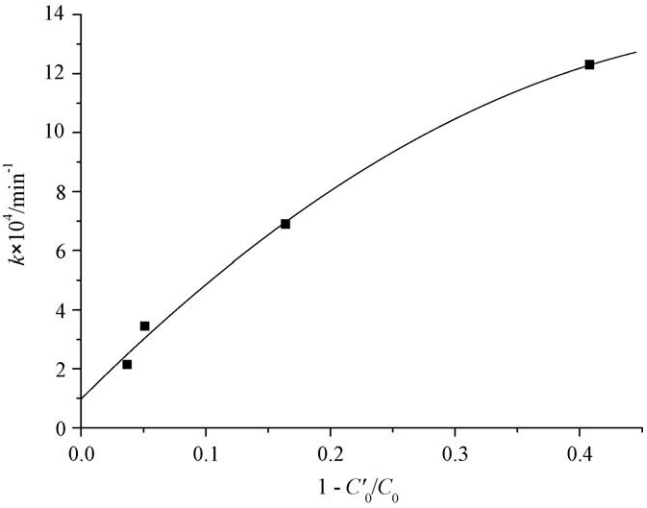

Fig. 12. Correlation of k with $1 - (C_0'/C_0)$.

Accordingly, the promotion of MB degradation on $Fe_{3-x}Ti_xO_4$ due to the introduction of Ti was mainly attributed to the pronounced increase of MB adsorbed on $Fe_{3-x}Ti_xO_4$. This result is not consistent with the reaction mechanism that the promotion of MB degradation on $Fe_{3-x}M_xO_4$ (M=Co, Mn and Cr) was attributed to promoting the decomposition of H_2O_2 [28–30].

4. Conclusion

MB can be degraded by $Fe_{3-x}Ti_xO_4$ in the presence of H_2O_2 at neutral pH values efficiently. This provides an effective magnetic heterogeneous Fenton catalyst which can conduct at neutral pH values. The heterogeneous reaction mechanism involves the adsorption of MB on $Fe_{3-x}Ti_xO_4$ and the catalytic decomposition of H_2O_2 by $Fe_{3-x}Ti_xO_4$ to form hydroxyl radical. The results provide an insight for heterogeneous Fenton reaction that in comparison with promoting the production of hydroxyl radical, the increase of organics adsorbed on catalyst may have the same effect on promoting the degradation of organic pollutants.

Acknowledgments

This work was financially supported by National Natural Science Foundation of China (Grant No. 40773060) and "863" Exploration Program, the Ministry of Science and Technology of the People's Republic of China (Grant No. 2006AA03Z337). This is contribution No. IS-1036 from GIGCAS.

References

[1] P. Baldrian, V. Merhautova, J. Gabriel, F. Nerud, P. Stopka, M. Hruby, M.J. Benes, Appl. Catal. B: Environ. 66 (2006) 258–264.
[2] F. Nerud, P. Baldrian, I. Eichlerova, V. Merhautova, J. Gabriel, L. Homolka, Biocatal. Biotransform. 22 (2004) 325–330.
[3] E. Torres, I. Bustos-Jaimes, S. Le Borgne, Appl. Catal. B: Environ. 46 (2003) 1–15.
[4] P. Baldrian, FEMS Microbiol. Rev. 30 (2006) 215–242.
[5] S.C. Zhang, Z.J. Zheng, J.H. Wang, J.M. Chen, Chemosphere 65 (2006) 2282–2288.
[6] F. Kiriakidou, D.I. Kondarides, X.E. Verykios, Catal. Today 54 (1999) 119–130.
[7] I. Poulios, E. Micropoulou, R. Panou, E. Kostopoulou, Appl. Catal. B: Environ. 41 (2003) 345–355.
[8] M. Stylidi, D.I. Kondarides, X.E. Verykios, Appl. Catal. B: Environ. 47 (2004) 189–201.
[9] P.C. Fung, K.M. Sin, S.M. Tsui, J. Soc. Dyers Colour. 116 (2000) 170–173.

[10] P.C. Fung, C.S. Poon, C.W. Chu, S.M. Tsui, Water Sci. Technol. 44 (2001) 67–72.
[11] E. Kusvuran, O. Gulnaz, S. Irmak, O.M. Atanur, H.I. Yavuz, O. Erbatur, J. Hazard. Mater. 109 (2004) 85–93.
[12] I.A. Balcioglu, I. Arslan, Water Sci. Technol. 43 (2001) 221–228.
[13] K. Dutta, S. Bhattacharjee, B. Chaudhuri, S. Mukhopadhyay, J. Environ. Sci. Health A 38 (2003) 1311–1326.
[14] S. Lee, J. Oh, Y. Park, Bull. Kor. Chem. Soc. 27 (2006) 489–494.
[15] J.A. Zazo, J.A. Casas, A.F. Mohedano, M.A. Gilarranz, J.J. Rodriguez, Environ. Sci. Technol. 39 (2005) 9295–9302.
[16] W.Z. Tang, R.Z. Chen, Chemosphere 32 (1996) 947–958.
[17] A. Kornmuller, S. Karcher, M. Jekel, Water Sci. Technol. 46 (2002) 43–50.
[18] J.Y. Feng, X.J. Hu, P.L. Yue, Environ. Sci. Technol. 38 (2004) 5773–5778.
[19] O.S.N. Sum, J.Y. Feng, X.J. Hu, P.L. Yue, Top. Catal. 33 (2005) 233–242.
[20] J.Y. Feng, X.J. Hu, P.L. Yue, Water Res. 39 (2005) 89–96.
[21] J.Y. Feng, X.J. Hu, P.L. Yue, Water Res. 40 (2006) 641–646.
[22] A.H. Gemeay, I.A. Mansour, R.G. El-Sharkawy, A.B. Zaki, J. Mol. Catal. A: Chem. 193 (2003) 109–120.
[23] W.P. Kwan, B.M. Voelker, Environ. Sci. Technol. 37 (2003) 1150–1158.
[24] B.W. Tyre, R.J. Watts, G.C. Miller, J. Environ. Qual. 20 (1991) 832–838.
[25] S.H. Kong, R.J. Watts, J.H. Choi, Chemosphere 37 (1998) 1473–1482.
[26] L.C.A. Oliveira, D.I. Petkowicz, A. Smaniotto, S.B.C. Pergher, Water Res. 38 (2004) 3699–3704.
[27] Y. Kim, B. Lee, J. Yi, Sep. Sci. Technol. 38 (2003) 2533–2548.
[28] F. Magalhaes, M.C. Pereira, S.E.C. Botrel, J.D. Fabris, W.A. Macedo, R. Mendonca, R.M. Lago, L.C.A. Oliveira, Appl. Catal. A: Gen. 332 (2007) 115–123.
[29] R.C.C. Costa, M. de Fatima, F. Lelis, L.C.A. Oliveira, J.D. Fabris, J.D. Ardisson, R. Rios, C.N. Silva, R.M. Lago, Catal. Commun. 4 (2003) 525–529.
[30] R.C.C. Costa, M.F.F. Lelis, L.C.A. Oliveira, J.D. Fabris, J.D. Ardisson, R. Rios, C.N. Silva, R.M. Lago, J. Hazard. Mater. 129 (2006) 171–178.
[31] P. Perriat, E. Fries, N. Millot, B. Domenichini, Solid State Ionics 117 (1999) 175–184.
[32] N. Guigue-Millot, Y. Champion, M.J. Hytch, F. Bernard, S. Begin-Colin, P. Perriat, J. Phys. Chem. B 105 (2001) 7125–7132.
[33] E.A. El-Sharkawy, A.Y. Soliffian, K.M. Al-Amer, J. Colloid Interf. Sci. 310 (2007) 498–508.
[34] R.M. Cornell, U. Schwertmann, The Iron Oxides: Structure, Properties, Reactions, Occurrences and Uses, Wiley-VCH, New York, 2003.
[35] W. Yu, T.L. Zhang, H. Zhang, X.J. Qiao, L. Yang, Y.H. Liu, Mater. Lett. 60 (2006) 2998–3001.
[36] T. Sugimoto, E. Matijevic, J. Colloid Interf. Sci. 74 (1980) 227–243.
[37] R.C. Wu, H.H. Qu, H. He, Y.B. Yu, Appl. Catal. B: Environ. 48 (2004) 49–56.
[38] J. He, W.H. Ma, J.J. He, J.C. Zhao, J.C. Yu, Appl. Catal. B: Environ. 39 (2002) 211–220.
[39] B.A. Wechsler, D.H. Lindsley, A.C. Prewitt, Am. Mineral. 69 (1984) 754–770.
[40] S. Cui, X.D. Shen, B.L. Lin, G.D. Jiang, W.H. Zhang, J. Wuhan Univ. Technol. 23 (2008) 436–439.
[41] J.T. Keiser, C.W. Brown, R.H. Heidersbach, J. Electrochem. Soc. 129 (1982) 2686–2689.
[42] G.W. Poling, J. Electrochem. Soc. 116 (1969) 958.
[43] S. Okamoto, J. Am. Ceram. Soc. 51 (1968) 594–599.
[44] P.S. Sidhu, R.J. Gilkes, A.M. Posner, Soil Sci. Soc. Am. J. 45 (1981) 641–644.
[45] H.H. Hamdeh, K. Barghout, J.C. Ho, P.M. Shand, L.L. Miller, J. Magn. Magn. Mater. 191 (1999) 72–78.
[46] Z. Kakol, J. Sabol, J.M. Honig, Phys. Rev. B 43 (1991) 649–654.
[47] R.R. Sheha, E. Metwally, J. Hazard. Mater. 143 (2007) 354–361.
[48] A. Houas, H. Lachheb, M. Ksibi, E. Elaloui, C. Guillard, J.M. Herrmann, Appl. Catal. B: Environ. 31 (2001) 145–157.
[49] H. Gnaser, M.R. Savina, W.F. Calaway, C.E. Tripa, I.V. Veryovkin, M.J. Pellin, Int. J. Mass. Spectrom. 245 (2005) 61–67.
[50] H. Ma, Q. Zhuo, B. Wang, Environ. Sci. Technol. 41 (2007) 7491–7496.
[51] R.P. Schwarzenbach, P.M. Gschwend, D.M. Imboden, Environmental Organic Chemistry, second ed., Wiley-Interscience, New Jersey, 2003.
[52] S.S. Lin, M.D. Gurol, Environ. Sci. Technol. 32 (1998) 1417–1423.
[53] S.S. Chou, C.P. Huang, Chemosphere 38 (1999) 2719–2731.
[54] R. Andreozzi, V. Caprio, R. Marotta, Water Res. 36 (2002) 2761–2768.
[55] R. Andreozzi, A. D'Apuzzo, R. Marotta, Water Res. 36 (2002) 4691–4698.
[56] W.P. Kwan, B.M. Voelker, Environ. Sci. Technol. 36 (2002) 1467–1476.
[57] J. He, W.H. Ma, W.J. Song, J.C. Zhao, X.H. Qian, S.B. Zhang, J.C. Yu, Water Res. 39 (2005) 119–128.